Int j simul model 23 (2024) 1, 77-88
Original scientific paper

WEAR SIMULATION OF THE CONVEYOR BELT TRANSFER CHUTE USING THE DEM

Lerher, T.; Grum, Z.; Motaln, M. & Zadravec, M.
University of Maribor, Faculty of Mechanical Engineering, Smetanova 17, 2000 Maribor, Slovenia
E-Mail: tone.lerher@um.si, z.grum94@gmail.com, marko.motaln2@um.si, matej.zadravec@um.si

Abstract
This paper presents a wear simulation-based performance evaluation of the conveyor belt transfer chute using the DEM (Discrete Element Method). Compared to known analytical and empirical wear models, DEM simulation can significantly increase the performance of wear analysis by enabling the analysis and optimization of highly complex geometries of material handling systems such as conveyor belt transfer chutes. Only the correct design of the conveyor belt transfer chute has the potential to significantly extend its service life, resulting in considerable cost savings. Based on the parametric analysis of different angles and radius in the upper head and lower section of the transfer chute, a new geometry of the transfer chute was proposed. The wear depth of the new conveyor belt transfer chute is compared with the wear resistant and low-carbon steel of the transfer chute along with the moderate and relatively high values of the solid granules mass flow. The results show that the wear depth of the transfer chute can be significantly reduced by using the wear-resistant steel compared to the low-carbon steel, which is significantly evident in high throughput rates of the solid granules mass flow.
(Received in September 2023, accepted in February 2024. This paper was with the authors 1 month for 1 revision.)

Key Words: Bulk Material Flow, Discrete Element Method (DEM), Transfer Chute Wear Simulation, Archard and Relative Wear, Performance Analysis

1. INTRODUCTION

Material handling represents one of the main industrial activities nowadays. Generally, we distinguish material handling systems for unit-load and bulk materials. One of the important material handling systems are conveyors, which are used for transport of materials between specific points over a fixed route. In practice, we distinguish different types of conveyors: belt conveyors, chain conveyors, screw conveyors, overhead chain conveyors, etc.

Belt conveyors are generally used for the transport of bulk materials, as they are simple in design and can economically transport large quantities of masses over long distances. Usually, they are equipped with a transfer chute configuration to efficiently transfer materials between two conveyor belts. Furthermore, transfer chutes redirect the flow from one conveyor to another, and discharge chutes ensure that the material leaving the conveyor effectively fills a bin, stockpile, truck, or wagon [1].

In the literature and in practice there are three types of transfer chute configurations: transfer chutes using impact plates, the rock box transfer chutes and dynamic chutes, also known as hood and spoon chutes. The name "hood and spoon" comes from the fact that this concept of the transfer chute involves a parabolic shaped, curved hood deflector at the top of the chute and a similar spoon deflector at the bottom of the chute to transfer the material onto the receiving belt [2]. This type of transfer chute improves the control of the material flow and is widely used in the minerals industry. Poorly designed conveyor belt transfer chutes can lead to considerable wear of the protective plates along with the damage or breakage of the conveyed goods, blockages at the discharge points, increased dust emissions, increased noise levels and damage to the receiving conveyor belt [3, 4].

Wear is the systematic removal of material from a surface through relative movement and contact between different surfaces. Both friction and wear are the result of a shared tribological contact process that occurs when two moving bodies interact. This phenomenon significantly

shortens the service life of the conveyor belt transfer chute. Proper design of the conveyor belt transfer chute has the potential to significantly extend its service life, resulting in considerable cost savings. As a rule, lower friction means a proportional reduction in the wear rate and vice versa. However, it is crucial to recognize that this principle is not universally applicable in every scenario [5].

Overcoming the challenges as wear, breakage, blockages, dust emissions, noise, etc. effectively requires a well thought-out design of the conveyor belt transfer chutes, the selection of appropriate materials of the transfer chute and strict adherence to the correct operating parameters for the conveyor belt system [6]. To extend the service life of the conveyor belt transfer chute, wear rate on transfer chutes belts must be minimized. The dynamics of bulk material flow influence the wear of transfer chutes and conveyor belts during transportation and underline their crucial role in influencing these factors [7]. In engineering, especially in the field of topology optimization [8], new geometries are often introduced to improve system performance.

A comprehensive understanding of the dynamics of particle motion is essential to increase the efficiency of the overall system and to ensure reliable redesign and optimization of transfer chutes. The current state of conveyor belt transfer chute design relies predominantly on empirical testing and the collective experience of engineers. In the past, researchers designing conveyor belt transfer chutes used a theoretical description based on partially derived analytical solutions. This method was effective for dealing with idealized geometries and simplified systems [9, 10]. However, the application of the new approaches to describe bulk material systems on an industrial level is often not possible. In practice, the consideration of bulk material systems is based on standards, empirical assessments, empirical values and findings from partial experiments [11].

Experiments are usually expensive and time-consuming. Nevertheless, the experiments are indispensable as they are often required to determine fundamental contact parameters and to calibrate numerical models [12]. With the rapid development of hardware capabilities, numerical simulation has become an attractive tool for the investigation and simulation of complex bulk material handling systems in scientific community. Discrete numerical methods are increasingly preferred and more appropriate, allowing for the analysis and optimization of highly complex conveyor geometries.

The beginnings of numerical modelling in material handling with a screw conveyor can be traced back to 2001, when Shimizu and Cundall [13] start applying DEM. Subsequent studies have investigated various aspects, including the mixing of granular media during transportation [14], granule flow and performance under different boundary conditions. A good example of using DEM in agriculture is the simulation analysis of the vertical screw stirring device for mixing and steering different types of fodders. By using DEM simulation, the authors identify the optimal parameters and confirm their results with an experiment [15]. Another interesting example of using DEM is the application of joint simulation with Multi Body Dynamics ADAMS. A simulation study on the dynamic properties of a chain-driven scraper conveyor for large coal was successfully implemented through the application of DEM and ADAMS [16].

The purpose of this paper is to evaluate conveyor belt transfer chute using discrete event simulation. The performance measure of the studied conveyor belt transfer chute is evaluated in terms of the Archard and relative wear model, which has an expressive influence on the service life of the transfer chute.

The remainder of the paper is organized as follows. In section 2, discrete element method is presented. In section 3, simulation model of the conveyor belt transfer chute is presented. Analysis of simulation results along with discussions are presented in section 4. Finally, in section 5, we provide main conclusions from this study.

2. DISCRETE ELEMENT METHOD

In recent decades, the Discrete Element Method (DEM) has become an effective tool for describing the motion of granular solids (particle materials); it is used in many areas, from mining to chemical and pharmaceutical industries.

DEM enables the numerical treatment of the motion of a large number of particles. In DEM, each particle is considered as individual, which moves completely independently. It is assumed that all particles are rigid bodies and that the interaction between them only takes place at the contact surface of these particles. The so-called soft contact approach is used on this contact surface, which means that an overlap (δ) between the particles at the contact points is permitted.

In DEM simulations, several contact and external forces (e.g. gravity) act on the particles and cause motion, which is calculated using Newton's second law of motion. The movement of the particles changes the contact conditions, which is reflected in the changing contact forces that constantly cause new movements of the particles. The DEM takes in account the translational and rotational motion equations of the particles, which is presented with Eqs. (1) and (2) [17]:

$$m_i\,\vec{a}_i = m_i\,\frac{d}{dt}\vec{v}_i = \sum_{j=1}^{nc}\vec{F}_{ij} + \vec{F}_i^{\,g} + \vec{F}_i^{\,ext} \tag{1}$$

$$I_i\;\vec{\vartheta}_i = I_i\;\;\frac{d}{dt}\vec{\omega}_i = \sum_{j=1}^{nc}\vec{T}_{ij} + \vec{T}_i^{\,rol} + \vec{T}_i^{\,ext} \tag{2}$$

The position of particles can be described using the position vectors $\vec{x}_i$. Similarly, rotation is described using the vector $\vec{\varphi}_i$. Where m_i is the mass of the designated particle, I_i is the corresponding moment of inertia. The translational motion of the particle can be described using the velocity vector $\vec{v}_i$, while the vector $\vec{a}_i$ represents the acceleration. Analogously, the angular velocity vector is denoted as $\vec{\omega}_i$, and the angular acceleration vector is denoted as $\vec{\vartheta}_i$. Arising from interactions with neighbouring particles, supplementary forces $\vec{F}_{ij}$ and moments $\vec{T}_{ij}$ result from the combined influence of all neighbouring contacts (*nc*). Additionally, external forces $\vec{F}_i^{\,ext}$ and moments $\vec{T}_i^{\,ext}$ can be considered including the gravitational field $\vec{F}_i^{\,g}$, and the rolling resistance $\vec{T}_i^{\,rol}$ between particles. For a timestep *t* contact C_{ij} between "non deformable" particles D_i and D_j can be illustrated as shown in Fig. 1.

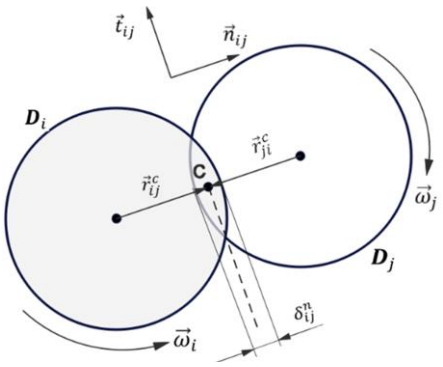

Figure 1: DEM contact representation between two "non deformable" spherical particles.

Introducing variables δ_{ij}^n and δ_{ij}^t to represent normal and tangential overlap, respectively, the "soft sphere" approach model deals with rigid particles simulating deformation through superposition. To determine the tangential overlap, an incremental approach is employed, with $\vec{v}_{rel}^{\,t}$ indicating the relative velocity in the tangential direction. Most DEM programs reported by the authors [18-21], calculate tangential overlap based on contact history.

2.1 Hertz – Mindlin (no slip) contact model

Normal contact is derived from the contributions of the physicist Hertz, while the description of tangential contact is credited to the collaborative efforts of Mindlin and Deresiewicz [5]. Two spherical particles contact each other elastically. The force acting on the particles in contact is given with the Eq. (3):

$$F_c = F_n + F_t \tag{3}$$

where F_c is the contact force, F_n is the normal contact force and F_t is the tangential contact force. For spherical particles, the normal contact force can be expressed with the Eq. (4) [21]:

$$F_{ij}^n = \frac{4}{3} E^* \sqrt{R^*}\, \delta^{n\,\frac{3}{2}} - 2\sqrt{\frac{5}{6}}\, \beta \sqrt{S_n\, m^*}\, \vec{v}_{rel}^{\,n} \tag{4}$$

where E^*, R^* and S_n are the equivalent Young's Modulus, equivalent particle radius and normal stiffness. Coefficient β can be directly connected to coefficient of restitution and can be calculated with the Eq. (5):

$$\beta = \frac{\ln(c_r)}{\sqrt{ln^2(c_r) + \pi^2}} \tag{5}$$

where c_r is the coefficient of restitution. Similarly, with the tangential stiffness S_t in Eq. (6):

$$S_t = 8G^* \sqrt{R^*\ \delta^t} \tag{6}$$

we can express the force in the tangential direction with the Eq. (7):

$$F_{ij}^t = -S_t \delta^t\ - 2\sqrt{\frac{5}{6}}\, \beta \sqrt{S_t\, m^*}\, \vec{v}_{rel}^{\,t} \tag{7}$$

where $\vec{v}_{rel}^{\,t}$ is the relative tangential velocity.

2.2 Archard wear model

The model is based on work by Archard [7], which suggests that the quantity of material removed from the surface is directly proportional to the frictional work performed by particles moving across the surface. Volume of the removed material Q can be expressed by the Archard wear Eq. (8) [18]:

$$Q = \frac{K}{H} \cdot F_n d_t \tag{8}$$

The Archard wear equation establishes a relationship between wear, normal load F_n sliding distance d_t, and material hardness H. Although the Archard wear expression represents a relatively simple model for wear prediction, its accuracy is limited by its dependence on the empirical wear constant K. This constant K is of critical importance but is inherently material and condition specific as it considers variables such as surface roughness, lubrication and environmental factors that influence wear rates. To improve prediction accuracy, engineers use experimental data and advanced calibration techniques to determine the Archard wear constant K for a given material pair under different operating conditions. As the Archard wear expression predicts a volume of material to be removed, it is rearranged to provide the depth per element, which is expressed with the Eq. (9):

$$h = \frac{Q}{A} \tag{9}$$

where h represents wear depth and A represents the surface.

2.3 Relative wear model

The relative wear model is a method for identifying regions of high impact (normal wear) and abrasion (tangential wear) on the transfer chute with a simulation. It is calculated based on the

relative velocity and associated forces between the particles and the transfer chute. This model provides a data that indicates the areas where wear is occurring in the transfer chute. While it provides quantitative values for comparison between two or more design iterations, it does not determine an explicit material removal rate. The four relative wear properties are the normal cumulative contact energy E_n, the tangential cumulative contact energy E_t, the normal cumulative force F_{nc} and the tangential cumulative force F_{tc}, which are presented in Eqs. (10) and (11).

$$E_n = \sum |F_n \cdot v_n \cdot \delta^n| \text{ and } E_t = \sum |F_t \cdot v_t \cdot \delta^t| \tag{10}$$

where v_n is the normal relative velocity and is negative in a loading situation, meanwhile v_t is the tangential relative velocity.

$$F_{nc} = \sum |F_n| \text{ and } F_{tc} = \sum |F_t| \tag{11}$$

where F_{nc} is the cumulative peak forces of the different contacts occurring on the geometry elements, meanwhile F_{tc} is the cumulative tangential forces and is dependent on the selected time step [22].

3. SIMULATION MODEL OF THE CONVEYOR BELT TRANSFER CHUTE

The simulation model of the conveyor belt transfer chute was developed in the Altair EDEM Academic software from 2020 [17]. Altair EDEM is high-performance software for the simulation of bulk solids and granulates.

Based on the DEM, Altair EDEM is able to calculate the forces acting on individual particles. Accelerations, velocities and positions of particles are calculated using Newton's laws of motion and numerical integration. Altair EDEM is able to quickly and accurately simulate and analyse the behaviour of various particles such as coal, mined ores, soils, fibres, grains, tablets, powders, etc. [17].

In continuation material properties, particle, and contact model along with the geometry of the conveyor belt transfer chute used in our simulation model will be presented.

3.1 Material properties

In order to carry out a DEM analysis, we need material data obtained experimentally through numerous tests. These relate to bulk density, shear modulus and Poisson's ratio. Since the individual materials are in contact when performing the DEM simulation, we also need to determine the coefficient of restitution, the coefficient of static and rolling friction.

An alternative to relatively expensive, time-consuming and complex experiments is the application of material properties of selected materials previously determined by other researchers. In our analysis, we used the values for the iron ore pellets material, the conveyor belt material and the transfer chute materials along with their interactions from the research of [23]. For the wear-resistant transfer chute material, we used the values from the study in [24].

Table I: Coefficients of materials used in simulations [23, 24].

Material	Properties		
	Density (kg/m^3)	Poisson's ratio	Shear modulus (Pa)
Wear-resistant steel (NM360)	7800	0.30	8.0×10^{10}
Low-carbon steel	7850	0.30	1.0×10^{10}
Rubber	4000	0.25	1.0×10^{6}
Iron ore pellets	3380	0.27	2.46×10^{7}

Table II: Contact parameters used in simulations [23].

Material interactions	Contact parameters		
	Coefficient of restitution	Coefficient of static friction	Coefficient of rolling friction
Iron ore pellets – Iron ore pellets	0.5	0.6	0.01
Iron ore pellets – Wear-resistant steel (NM360)	0.5	1.05	0.01
Iron ore pellets – Low-carbon steel	0.5	1.2	0.01

3.2 Particle model

The iron ore pallets present shapes that approach spheres. The Altair EDEM can simulate the typical iron ore particle shapes by accumulating several small spheres. The closer the particle model is to the real particles, the more accurate the results. However, too many spheres significantly reduce the efficiency of the calculation. In our analysis, the diameters of the iron ore pellets (spheres) varied between 15 and 20 mm. There are 10 % of particles with a diameter of less than 15 mm and 10 % of particles with a diameter of more than 20 mm.

Table III: Particle size of bulk material [23].

Particles	Particle diameter (mm)			
	< 15	15	20	> 20
Size distribution (%)	10	40	40	10

3.3 Contact model

In our research study, the Hertz–Mindlin model [18] with Archard [7] and Relative wear contact models were used for the interaction between particles and geometry (see section 2). The parameters related to the EDEM material properties and the contact parameters were set as listed in section 3.1. The wear constant between the friction pairing of the iron ore pellets and the wear-resistant steel (NM360) was 8×10^{-13} m^2/N. The wear constant between the friction pairing of iron ore pellets and low-carbon steel was $6{,}5 \times 10^{-12}$ m^2/N [25].

3.4 Geometry of the conveyor belt transfer chute

The proposed conveyor belt transfer chute was designed based on the current designs available in the literature [26] .The complete conveyor belt transfer chute system consists of the (upper) discharging conveyor belt, the transfer chute and the (bottom) receiving conveyor belt (Fig. 2 a). The discharging conveyor belt is driven by a drive roller with a diameter of 300 mm and has a width of 650 mm. The receiving conveyor belt has a width of 650 mm. The height between the discharging and the receiving conveyor has been set at 1650 mm. The width of the upper head chute was set at 700 mm (Fig. 2 b).

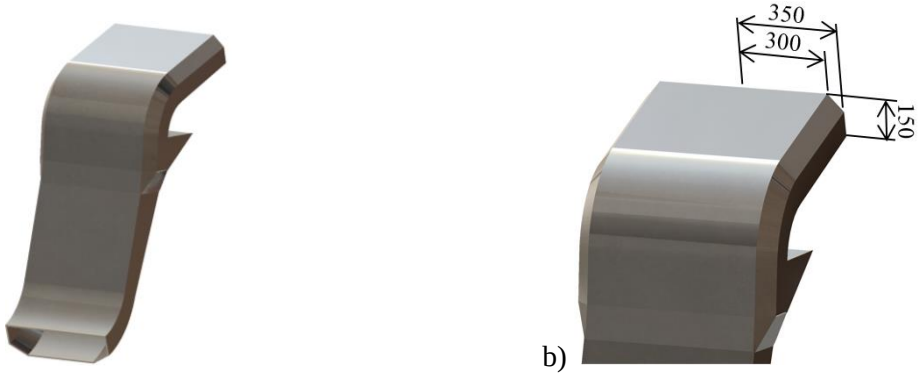

Figure 2: a) 3D model of the conveyor belt transfer chute; b) Dimensions of the transfer chute upper head given in millimetres [25].

The conveyor belt transfer chute system (Fig. 3) was designed using the upper and lower curve deflector, i.e. the hood and the spoon transfer chute. The plate thickness of the transfer chute was set at 10 mm [26].

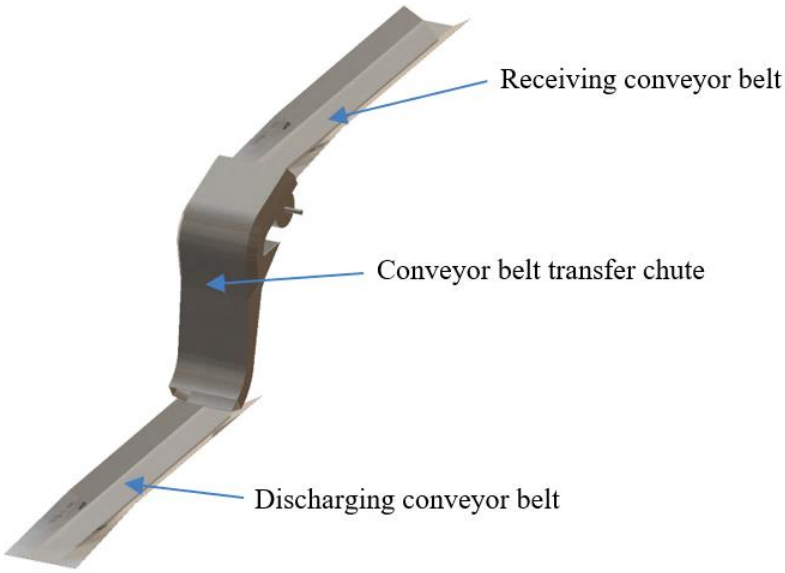

Figure 3: The conveyor belt transfer chute system [25].

4. CASE STUDY

This section presents and discusses the most important results of the wear analysis for the conveyor belt transfer chute. The velocity of the iron ore particles was set to v = 3 m/s and the mass flow rate to q = 30 kg/s. The particles are generated on a surface 400 mm wide and 200 mm high. The particles are only generated with an initial velocity in the horizontal direction.

Eulerian time integration with a fixed time step of 20 % (5.99×10^{-5} s) was used. The total simulation time was set to T = 60.5 seconds. Target save interval was set to 0.05 seconds with 1.21×10^3 data points. Regarding the simulator grid the smallest radius R_{min} was 7.5 mm, which gives us the estimated cell size of 18.75 mm ($2.5 \cdot R_{min}$). The estimated number of cells was 1.94922×10^6. We used the CPU solver with 8 CPU cores for the simulation engine.

Other related data (material properties, particle and contact model as well as the geometry of the conveyor belt transfer chute) are presented in section 3.

4.1 Wear parametric analysis of the conveyor belt transfer chute

The wear parametric analysis was carried out on the hood (upper head chute) and on the spoon (lower chute) of the conveyor belt transfer chute (Fig. 4 a). With the objective of obtaining the smallest possible wear depth at the transfer chute, we have changed the angle in the upper head chute and the hood radius (Fig. 4 b). As well, we have changed the angle in the lower chute and the spoon radius of the transfer chute (Fig. 4 b).

Tables IV and V show the results of the wear parametric analysis of the conveyor belt transfer chute. The maximum and total wear depth as well as the normal and tangential cumulative contact energy are highly dependent on the geometry (angle and radius) of the conveyor belt transfer chute.

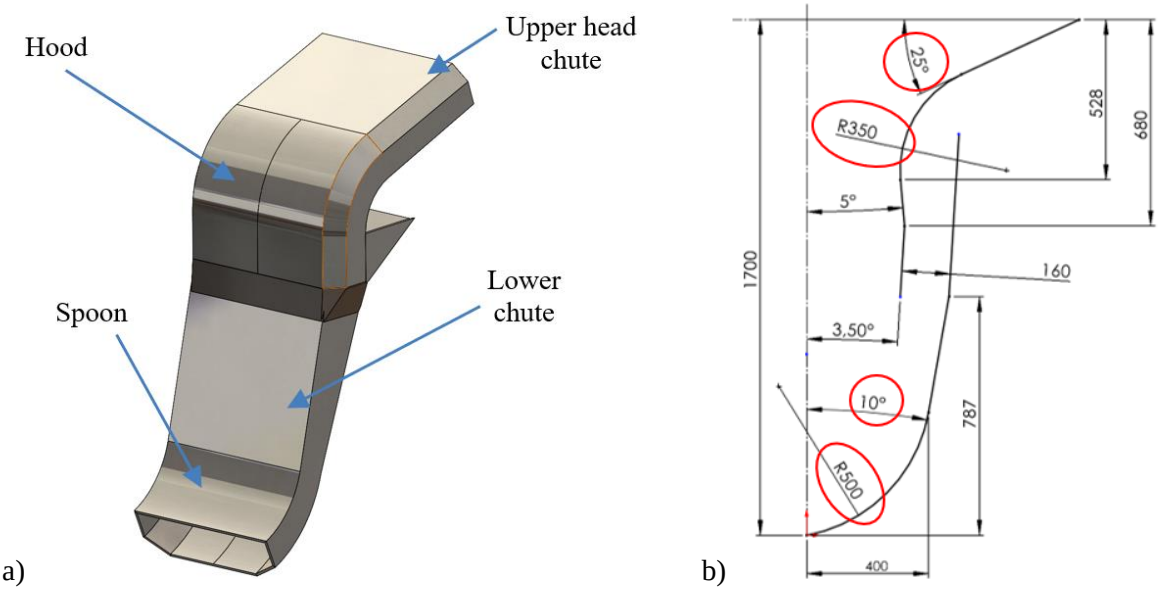

Figure 4: a) 3D model of the upper head chute and lower chute; b) Dimensions of the conveyor belt transfer chute given in millimetres [25].

Table IV: Results of the wear analysis in the upper head chute (Hood).

Hood – upper head chute					
Angle in the upper head chute (degrees)	Archard wear (mm)		Relative wear (J)		Velocity (m/s)
	Max. wear depth	Total wear depth	Normal cumulative contact energy	Tangential cumulative contact energy	Average particle velocity
15	3.81×10^{-5}	1.15×10^{-3}	2135.6	6540.8	3.37
17.5	3.20×10^{-5}	9.67×10^{-4}	1475.2	6002.7	3.20
20	$\mathbf{2.90 \times 10^{-5}}$	$\mathbf{8.10 \times 10^{-4}}$	**1472.6**	**6151.7**	**3.42**
22.5	3.27×10^{-5}	7.87×10^{-4}	1501.6	6018.0	3.42
25	3.62×10^{-5}	7.59×10^{-4}	1589.0	6009.3	3.40
27.5	3.51×10^{-5}	8.13×10^{-4}	1765.8	6096.1	3.38
30	4.79×10^{-5}	8.54×10^{-4}	1980.1	6144.9	3.38
Hood radius (mm)	Archard wear (mm)		Relative wear (J)		Velocity (m/s)
	Max. wear depth	Total wear depth	Normal cumulative contact energy	Tangential cumulative contact energy	Average particle velocity
300	3.39×10^{-5}	8.67×10^{-4}	1518.9	6058.7	3.46
325	3.08×10^{-5}	8.46×10^{-4}	1497.0	6100.0	3.45
350	$\mathbf{2.90 \times 10^{-5}}$	$\mathbf{8.10 \times 10^{-4}}$	**1472.6**	**6151.7**	**3.42**
375	3.01×10^{-5}	8.35×10^{-4}	1428.2	6108.6	3.41
400	3.13×10^{-5}	8.11×10^{-4}	1421.4	6159.0	3.39

Note for Tables IV and V: The maximum wear depth values represent the maximum wear that occurs at a specific point on the surface. The total wear value represents the sum of the wear over the entire surface that was generated in the simulation.

According to the distribution of the angle α = (15, 17.5, 20, 22.5, 25, 27.5, 30˚) in the upper head chute, the acceptable wear depth results at an angle of α = 20˚. Based on the distribution of the hood radius R_{hood} = (300, 325, 350, 375, 400 mm), the acceptable wear depth is given by the hood radius R_{hood} = 350 mm.

Table V: Results of the wear analysis in the lower chute (Spoon).

Spoon – lower chute					
Angle in the lower chute (degrees)	Archard wear (mm)		Relative wear (J)		Velocity (m/s)
	Max. wear depth	Total wear depth	Normal cumulative contact energy	Tangential cumulative contact energy	Average particle velocity
8	7.41×10^{-5}	3.00×10^{-3}	3909.1	13860.1	2.84
10	5.50×10^{-5}	2.44×10^{-3}	3981.7	13656.3	2.85
12	4.32×10^{-5}	2.23×10^{-3}	4136.7	13658.1	2.8
14	$\mathbf{4.11 \times 10^{-5}}$	$\mathbf{2.07 \times 10^{-3}}$	**4439.5**	**13715.2**	**2.76**
16	4.52×10^{-5}	2.16×10^{-3}	4878.7	13784.7	2.70
Spoon radius (mm)	Archard wear (mm)		Relative wear (J)		Velocity (m/s)
	Max. wear depth	Total wear depth	Normal cumulative contact energy	Tangential cumulative contact energy	Average particle velocity
400	4.56×10^{-5}	2.23×10^{-3}	4774.8	13736	3.11
450	4.28×10^{-5}	1.82×10^{-3}	4417.6	13527.7	3.21
500	$\mathbf{4.09 \times 10^{-5}}$	$\mathbf{1.58 \times 10^{-3}}$	**4126.8**	**13366.9**	**3.27**
550	4.09×10^{-5}	1.47×10^{-3}	3933.0	13112.8	3.34
600	4.10×10^{-5}	1.46×10^{-3}	3747.4	13016.5	3.38

According to the distribution of the angle β = (8, 10, 12, 14, 16˚) in the lover chute, the acceptable (minimal) wear depth results at an angle of β = 14˚. Based on the distribution of the spoon radius R_{spoon} = (400, 450, 500, 550, 600 mm), the acceptable wear depth is given by the spoon radius R_{spoon} = 500 mm.

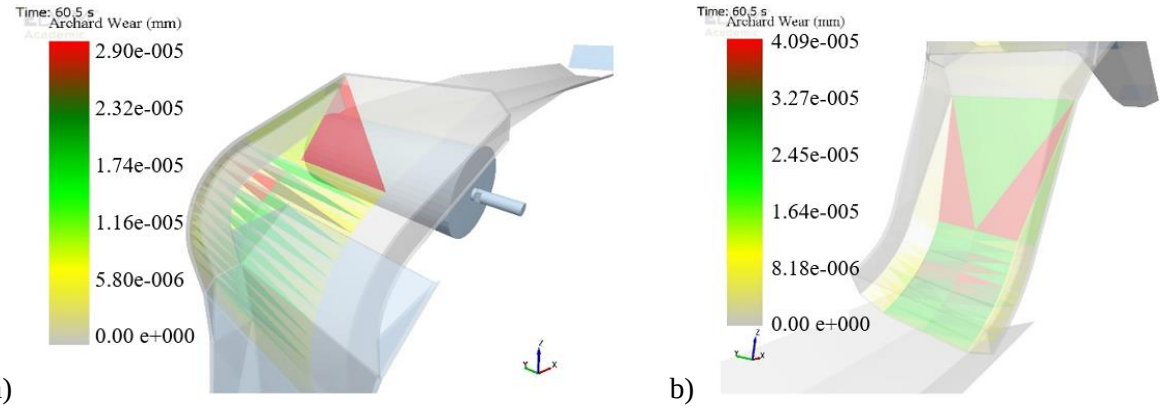

a) b)

Figure 5: Areas of the max. wear of the conveyor belt transfer chute; a) upper head chute (Hood), b) lower chute (Spoon) [25].

The wear depth distributions of the conveyor belt transfer chute are shown in Figs. 5 a and 5 b. It was found that abrasive wear is localized in areas where the material flow exerts high pressure on the plate surface, while erosive wear occurs in areas where the impact velocity and frequency of the particles is high or where the impact angle is oblique.

Based on the results presented in Tables IV and V, a new geometry of the conveyor belt transfer chute was proposed (Figs. 6 a and 6 b).

4.2 Wear analysis of the conveyor belt transfer chute based on mass flow

In the wear simulation of the conveyor belt transfer chute as a function of the mass flow, we changed the mass flow of the particles and the material of the transfer chute. We used wear-

resistant steel (NM360) and low-carbon steel for the material of the transfer chute (see section 3). In the simulation analysis, we used a new geometry of the conveyor belt transfer chute presented on Figs. 6 a and 6 b.

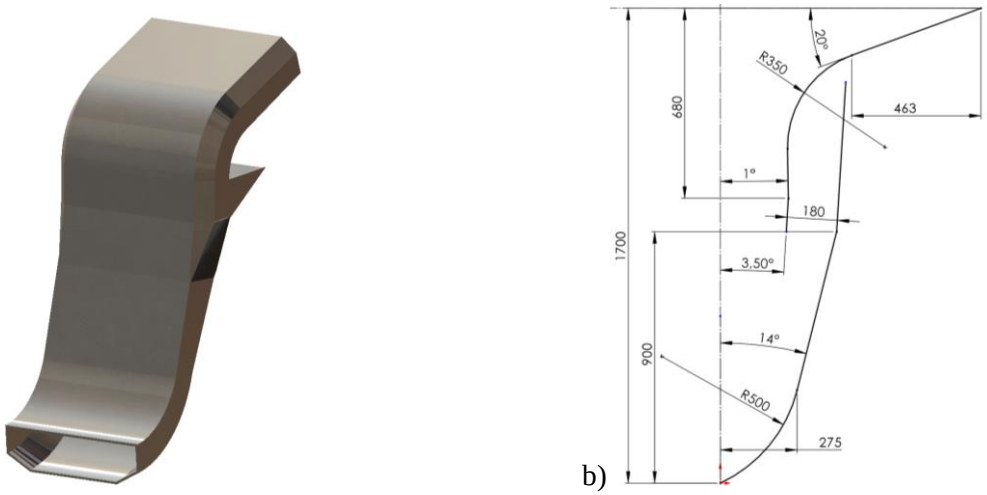

Figure 6: a) 3D model of the new conveyor belt transfer chute; b) Dimensions of the new conveyor belt transfer chute given in millimetres [25].

Table VI: Results of the wear analysis based on mass flow and transfer chute material (steel).

Hood – upper head chute					
Mass flow (kg/s)	Archard wear (mm)				Average particle velocity (m/s)
	Wear-resistant steel (NM360)		Low-carbon steel		
	Max. wear depth	Total wear depth	Max. wear depth	Total wear depth	
10	8.52×10^{-6}	1.71×10^{-4}	5.50×10^{-5}	1.19×10^{-3}	3.67
20	1.60×10^{-5}	4.22×10^{-4}	1.16×10^{-4}	3.13×10^{-3}	3.45
30	2.41×10^{-5}	7.34×10^{-4}	1.58×10^{-4}	5.57×10^{-3}	3.31
40	2.88×10^{-5}	1.03×10^{-3}	2.20×10^{-4}	7.96×10^{-3}	3.29
50	3.89×10^{-5}	1.38×10^{-3}	3.14×10^{-4}	1.07×10^{-2}	3.27
60	5.02×10^{-5}	1.79×10^{-3}	4.11×10^{-4}	1.40×10^{-2}	3.24
Spoon – lower chute					
Mass flow (kg/s)	Archard wear (mm)				Average particle velocity (m/s)
	Wear-resistant steel (NM360)		Low-carbon steel		
	Max. wear depth	Total wear depth	Max. wear depth	Total wear depth	
10	2.34×10^{-5}	3.67×10^{-4}	1.73×10^{-4}	2.53×10^{-3}	3.63
20	3.25×10^{-5}	8.98×10^{-4}	2.39×10^{-4}	6.83×10^{-3}	3.47
30	3.75×10^{-5}	1.53×10^{-3}	2.72×10^{-4}	1.17×10^{-2}	3.29
40	4.80×10^{-5}	2.15×10^{-3}	3.56×10^{-4}	1.67×10^{-2}	3.15
50	5.44×10^{-5}	2.79×10^{-3}	4.50×10^{-4}	2.15×10^{-2}	3.04
60	6.41×10^{-5}	3.33×10^{-3}	5.12×10^{-4}	2.58×10^{-2}	2.96

According to the wear depth distributions, the mass flow has a significant influence on the maximum and total wear depths for the upper and lower chute. When comparing the upper head chute and the lower chute, the wear depth is higher in the lower chute. The material of the transfer chute also has a significant influence on the maximum and total wear depths. The wear depth distributions are significantly lower in the case of wear-resistant steel (NM360) compared to low-carbon steel, which has an influence on the service life of the conveyor belt transfer

chute. Generally, the best results are achieved by using the wear-resistant steel (NM360) and moderate mass flows.

4. CONCLUSION

This paper presents Archard and relative wear simulation of the conveyor belt transfer chute using the Discrete Element Method (DEM). A parametric study based on DEM simulations was proposed to determine the best design of the conveyor belt transfer chute. First, a simulation model of the conveyor belt transfer chute was developed identifying the material properties of the transfer chute and solid granules, particle and the contact models, and the geometry of the transfer chute. The design of experiments was performed using a software tool Altair EDEM. Factors influencing the distribution of wear depth were angle and radius in the upper head (α, R_{hood}) and lower section (β, R_{spoon}) of the transfer chute. The performance measures were considered as follows: (*i*) Archard wear with maximum and total depth, (*ii*) Relative wear with normal and tangential cumulative contact energy, and (*iii*) Average particle velocity. The results of the parametric study are summarized in Tables V and VI. The best solution in the upper head of the conveyor belt transfer chute is at an angle of $\alpha = 20^{\circ}$ and the hood radius $R_{\text{hood}} = 350$ mm, where the level of maximum wear depth according to Archard is the smallest. The best solution in the lower section of the conveyor belt transfer chute is at an angle of $\beta = 14^{\circ}$ and the spoon radius $R_{\text{spoon}} = 500$ mm, where the level of maximum wear depth according to Archard is the smallest. Based on the parametric analysis in the upper head and lower section of the transfer chute, a new geometry of the conveyor belt transfer chute was proposed. Further wear analyses were carried out for the new geometry of the conveyor belt transfer chute with alternative material (wear-resistant and low-carbon steel) with the moderate and relatively high values of mass flow. In general, the lowest wear depth distributions were found for wear-resistant steel and moderate mass flows for both the upper head and lower section of the transfer chute. Generally, when deciding for the conveyor belt transfer chute, a DEM simulation can provide relatively fast and reliable data on the maximum and total depth wear distributions, which have an influence on the service life and thus on the cost savings.

This study can be extended in many directions. For example: (*i*) application of different solid granules, (*ii*) application of different configurations of conveyor belt transfer chutes with wear-resistant and low-carbon steel, (*iii*) application of different contact models such as the Hertz-Mindlin with JKR model may also be considered in the analysis.

REFERENCES

[1] Ilic, D.; Katterfeld, A. (2023). Simulation of transfer chutes, McGlinchey, D. (Ed.), *Simulations in Bulk Solids Handling: Applications of DEM and other Methods*, Wiley-VCH, Weinheim, 41-78, doi:10.1002/9783527835935.ch2

[2] Benjamin, C. W.; Huque, S. T.; Donecker, P.; Rozentals, J. J. (2010). *The Transfer Chute Design Manual: For Conveyor Belt Systems*, Conveyor Transfer Design Pty. Limited, Sydney

[3] Xie, L.; Zhong, W.; Zhang, H.; Yu, A.; Qian, Y.; Situ, Y. (2016). Wear process during granular flow transportation in conveyor transfer, *Powder Technology*, Vol. 288, 65-75, doi:10.1016/j.powtec.2015.10.043

[4] Ilic, D. (2019). Development of design criteria for reducing wear in iron ore transfer chutes, *Wear*, Vol. 434-435, Paper 202986, 13 pages, doi:10.1016/j.wear.2019.202986

[5] Wang, Q. J.; Zhu, D. (2013). Hertz theory: contact of spherical surfaces, Wang, Q. J.; Chung, Y.-W. (Eds.), *Encyclopedia of Tribology*, Springer, Boston, 1654-1662, doi:10.1007/978-0-387-92897-5_492

[6] Zhao, R.; Guo, L.; Gao, W.; Xiao, X.; Liu, Y. (2022). Structure optimization design of screw conveyor based on EDEM, *Journal of Physics: Conference Series*, Vol. 2200, Paper 012002, 9 pages, doi:10.1088/1742-6596/2200/1/012002

[7] Roessler, T.; Katterfeld, A. (2023). Calibrated and validated wear prediction for bulk material handling equipment using DEM simulations, *14th International Conference on Bulk Materials Storage, Handling and Transportation*, 284-295
[8] Glamsch, J.; Deese, K.; Rieg, F. (2019). Methods for increased efficiency of FEM-based topology optimization, *International Journal of Simulation Modelling*, Vol. 18, No. 3, 453-463, doi:10.2507/IJSIMM18(3)482
[9] Fruchtbaum, J. (2013). *Bulk Materials Handing Handbook*, Springer Science & Business Media, New York, doi:10.1007/978-1-4757-4695-2
[10] McGlinchey, D. (2008). *Bulk Solids Handling: Equipment Selection and Operation*, John Wiley & Sons, Hoboken
[11] Potrč, I. (1999). *Transport Systems*, Faculty of Mechanical Engineering, Maribor (in Slovenian)
[12] Blais, B.; Vidal, D.; Bertrand, F.; Patience, G. S.; Chaouki, J. (2019). Experimental methods in chemical engineering: discrete element method – DEM, *The Canadian Journal of Chemical Engineering*, Vol. 97, No. 7, 1964-1973, doi:10.1002/cjce.23501
[13] Shimizu, Y.; Cundall, P. A. (2001). Three-dimensional DEM simulations of bulk handling by screw conveyors, *Journal of Engineering Mechanics*, Vol. 127, No. 9, 864-872, doi:10.1061/(ASCE)0733-9399(2001)127:9(864)
[14] Pezo, L.; Jovanović, A.; Pezo, M.; Čolović, R.; Lončar, B. (2015). Modified screw conveyor-mixers – discrete element modeling approach, *Advanced Powder Technology*, Vol. 26, No. 5, 1391-1399, doi:10.1016/j.apt.2015.07.016
[15] Cao, K.; Li, X. H.; Gao, H. D.; Zhang, L. X.; You, F. (2023). Design and analysis of a vertical screw stirring device for feeding dairy goats, *International Journal of Simulation Modelling*, Vol. 22, No. 3, 462-473, doi:10.2507/IJSIMM22-3-655
[16] Jiang, S. B.; Huang, S.; Zeng, Q. L.; Wang, C. L.; Gao, K. D.; Zhang, Y. Q. (2022). Dynamic properties of chain drive system considering multiple impact factors, *International Journal of Simulation Modelling*, Vol. 21, No. 2, 284-295, doi:10.2507/IJSIMM21-2-603
[17] Altair Engineering Inc. Altair EDEM: Discrete Element Method (DEM) Software, from *https://altair.com/edem*, accessed on 01-01-2024
[18] Golshan, S.; Munch, P.; Gassmöller, R.; Kronbichler, M.; Blais, B. (2022). Lethe-DEM: an open-source parallel discrete element solver with load balancing, *Computational Particle Mechanics*, Vol. 10, No. 1, 77-96, doi:10.1007/s40571-022-00478-6
[19] Weinhart, T.; Orefice, L.; Post, M.; van Schrojenstein Lantman, M. P.; Denissen, I. F. C.; Tunuguntla, D. R.; Tsang, J. M. F.; Cheng, H.; Shaheen, M. Y.; Shi, H.; Rapino, P.; Grannonio, E.; Losacco, N.; Barbosa, J.; Jing, L.; Alvarez Naranjo, J. E.; Roy, S.; den Otter, W. K.; Thornton, A. R. (2020). Fast, flexible particle simulations – an introduction to MercuryDPM, *Computer Physics Communications*, Vol. 249, Paper 107129, 18 pages, doi:10.1016/j.cpc.2019.107129
[20] ANSYS Inc. ANSYS Rocky: Particle Dynamics Simulation Software, from *https://rocky.esss.co/*, accessed on 22-03-2023
[21] Altair Engineering Inc. Altair EDEM 2022: Getting Started, from *https://2022.help.altair.com/2022/EDEM/*, accessed on 27-11-2023
[22] Altair Engineering Inc. Altair EDEM 2022: Introducing EDEM, from *https://2022.help.altair.com/2022.2/EDEM/*, accessed on 01-01-2024
[23] Yang, G.; Li, Y.; Chen, D. (2015). Analysis of reclaiming process of bucket wheel stacker reclaimer based on DEM simulation, Zu, Q.; Hu, B.; Gu, N.; Seng, S. (Eds.), *Human Centered Computing (HCC 2014), Lecture Notes in Computer Science*, Springer, Cham, 69-79, doi:10.1007/978-3-319-15554-8_6
[24] Xia, R.; Wang, X.; Li, B.; Wei, X.; Yang, Z. (2019). Discrete element method (DEM) based study on the wear mechanism and wear regularity in scraper conveyor chutes, *Mathematical Problems in Engineering*, Vol. 2019, Paper 4191570, 12 pages, doi:10.1155/2019/4191570
[25] Grum, Ž. (2020). *Design and Numerical Analysis of Sheet Metal Wear of Belt Conveyor Transfer Chutes Using DEM Method*, Master Thesis, University of Maribor, Faculty of Mechanical Engineering, Maribor (in Slovenian)
[26] Katterfeld, A.; Donohue, T.; Ilic, D. (2012). Application of the discrete element method in mechanical conveying of bulk materials, *7th International Conference for Conveying and Handling of Particulate Solids (CHoPS 2012)*, 14 pages